Supplemental material for: Superconductivity-enhanced magnetic field noise

Shane P. Kelly and Yaroslav Tserkovnyak
Department of Physics and Astronomy and Mani L. Bhaumik Institute for Theoretical Physics, University of California, Los Angeles, CA 90095

CONTENTS

I. NV PROBE OF MATERIAL NOISE

The mode of NV relaxometry we consider is the T_1 noise spectroscopy similar to Refs [1–11]. In this mode, the NV is prepared, by optical driving, in an excited state, and is allowed to relax to its equilibrium state. The relaxation dynamics is then probed by optical read out, and the relaxation rate is determined based on the decay of the excited state. The relaxation is due to the noisy magnetic environment, and in a weak coupling approximation is determined by

$$T_1^{-1} = \left(\frac{g_{\rm nv}\mu_B}{2\hbar}\right)^2 \int_{-\infty}^{\infty} dt e^{i\omega t} \left\langle \left\{ B^- \left(\boldsymbol{r}_{\rm nv}, t\right), B^+ \left(\boldsymbol{r}_{\rm nv}, 0\right)\right\}\right\rangle , \tag{1}$$

as introduced in the main text.

In this appendix, we relate the stray magnetic fields produced outside the material to the current and magnetization density inside the material. Similar calculations have been performed in Refs [1, 11, 12], and so we summarize the essential assumptions and aspects of the calculation for completeness. Our main interest is the magnetic field at position $\boldsymbol{r}_{\rm nv} = \hat{\boldsymbol{z}}d + \boldsymbol{\rho}$ away from a slab of thickness L_z centered around $z = 0$. Here the position is outside the material $d > L_z/2$, and $\boldsymbol{\rho}$ is the position in the x-y plane. For both magnetization and current sources we make use of the Fourier transform:

$$\frac{1}{|\boldsymbol{r}_{\rm nv} - \boldsymbol{r}|} = \frac{1}{2\pi}\int \frac{d^2\boldsymbol{k}}{k} e^{-k|d-\hat{\boldsymbol{z}}\cdot\boldsymbol{r}|} e^{i\boldsymbol{k}\cdot(\boldsymbol{\rho}_{\rm nv}-\boldsymbol{\rho})}. \tag{2}$$

A. Demagnetization kernel

Assuming zero free current, the magnetic field is related to the magnetization via

$$\boldsymbol{\nabla}\cdot\boldsymbol{H} = -4\pi\boldsymbol{\nabla}\cdot\boldsymbol{M}, \tag{3}$$

which is equivalent to

$$\boldsymbol{B}(\boldsymbol{r}_{\rm nv}) = -\int_{\mathcal{R}_3} d^3\boldsymbol{r}\boldsymbol{\nabla}_{\boldsymbol{r}_{\rm nv}}\left(\boldsymbol{\nabla}_{\boldsymbol{r}}\frac{1}{|\boldsymbol{r}_{\rm nv}-\boldsymbol{r}|}\right)\cdot\boldsymbol{M}(\boldsymbol{r}) \tag{4}$$

for fields outside the material. Using the above relation we obtain

$$\boldsymbol{B}(\boldsymbol{r}_{\rm nv}) = -\frac{1}{2\pi}\int_{\mathcal{R}_2} d^2\boldsymbol{k}\int_{\mathcal{R}_3} dzd^2\boldsymbol{\rho}\frac{e^{-k|d-z|}}{k}e^{i\boldsymbol{k}\cdot(\boldsymbol{\rho}_{\rm nv}-\boldsymbol{\rho})}\left(k\hat{\boldsymbol{z}}-i\boldsymbol{k}\right)\left(-k\hat{\boldsymbol{z}}+i\boldsymbol{k}\right)\cdot\boldsymbol{M}(\boldsymbol{r}), \tag{5}$$

where we have used $\mathrm{sign}(d-z)=1$ as the NV is above the slab. Generally, for arbitrary d, the above equation holds under the following replacement:

$$\left(k\hat{\boldsymbol{z}}-i\boldsymbol{k}\right)\left(-k\hat{\boldsymbol{z}}+i\boldsymbol{k}\right)\to\left(k\hat{\boldsymbol{z}}\,\mathrm{sign}\left(d-z\right)-i\boldsymbol{k}\right)\left(k\delta\left(d-z\right)\hat{\boldsymbol{z}}-k\hat{\boldsymbol{z}}\,\mathrm{sign}(d-z)+i\boldsymbol{k}\right). \tag{6}$$

Assuming the magnetization is homogeneous in the $\hat{\boldsymbol{z}}$ direction: $\boldsymbol{M}=\boldsymbol{M}_2(\boldsymbol{\rho})\theta(L_z/2-|z|)/L_z$, we can perform the integral over z:

$$\boldsymbol{B}(\boldsymbol{r}_{\rm nv}) = \frac{1}{L_z\pi}\int_{\mathcal{R}_2} d^2\boldsymbol{k}\int_{\mathcal{R}_2} d^2\boldsymbol{\rho}e^{-kd}\sinh(L_zk/2)e^{i\boldsymbol{k}\cdot(\boldsymbol{\rho}_{\rm nv}-\boldsymbol{\rho})}\left(\hat{\boldsymbol{z}}-i\hat{\boldsymbol{k}}\right)\left(\hat{\boldsymbol{z}}-i\hat{\boldsymbol{k}}\right)\cdot\boldsymbol{M}_2(\boldsymbol{\rho}). \tag{7}$$

We therefore write the kernel in momentum space as

$$\hat{\boldsymbol{G}}_M(\boldsymbol{q},d) = 4\pi L_z^{-1}e^{-qd}\sinh(L_zq/2)\left(\mathrm{sign}(d)\hat{\boldsymbol{z}}-i\hat{\boldsymbol{q}}\right)\left(\mathrm{sign}(d)\hat{\boldsymbol{z}}-i\hat{\boldsymbol{q}}\right) \tag{8}$$

such that

$$\boldsymbol{B}(\boldsymbol{r}_{\rm nv}) = \int_{\mathcal{R}_2}\frac{d^2\boldsymbol{q}}{(2\pi)^2}e^{i\boldsymbol{q}\cdot\boldsymbol{\rho}_{\rm nv}}\hat{\boldsymbol{G}}_M(\boldsymbol{q},d)\cdot\boldsymbol{M}_2(\boldsymbol{q}), \tag{9}$$

where

$$\boldsymbol{M}_2(\boldsymbol{q}) = \int_{\mathcal{R}_2} d^2\boldsymbol{\rho}e^{-i\boldsymbol{q}\cdot\boldsymbol{\rho}}\boldsymbol{M}_2(\boldsymbol{\rho}). \tag{10}$$

The kernel is cutoff at a scale $q>1/d$. Thus, for a thin material, $L_z\ll d$, we have $q<1/d\ll 1/L_z$ and can approximate $L_zq\ll 1$. This gives the kernel:

$$\hat{\boldsymbol{G}}_M(\boldsymbol{q},d) = 2\pi qe^{-qd}\left(\mathrm{sign}(d)\hat{\boldsymbol{z}}-i\hat{\boldsymbol{q}}\right)\left(\mathrm{sign}(d)\hat{\boldsymbol{z}}-i\hat{\boldsymbol{q}}\right) \tag{11}$$

B. Oersted kernel

The magnetic field contributions from the free currents are given by the Oersted kernel

$$\boldsymbol{B}(\boldsymbol{r}_{\rm nv}) \;=\; \frac{1}{c}\int_{\mathcal{R}_3} d^3\boldsymbol{r}\frac{\boldsymbol{J}(\boldsymbol{r})\times(\boldsymbol{r}_{\rm nv}-\boldsymbol{r})}{|\boldsymbol{r}_{\rm nv}-\boldsymbol{r}|^3} = -\frac{1}{c}\int_{\mathcal{R}_3} d^3\boldsymbol{r}\boldsymbol{J}(\boldsymbol{r})\times\boldsymbol{\nabla}_{\boldsymbol{r}_{\rm nv}}\frac{1}{|\boldsymbol{r}_{\rm nv}-\boldsymbol{r}|}. \tag{12}$$

Substituting the Fourier transform above and again assuming a homogeneous distribution in the $\hat{\boldsymbol{z}}$ direction, $\boldsymbol{J}(\boldsymbol{r})=\boldsymbol{J}_2(\boldsymbol{r})\theta(|z|-L_z/2)/L_z$, we obtain the relation

$$\boldsymbol{B}(\boldsymbol{r}_{\rm nv})) = \int_{\mathcal{R}_2}\frac{d^2\boldsymbol{q}}{(2\pi)^2}e^{i\boldsymbol{q}\cdot\boldsymbol{r}_{\rm nv}}\boldsymbol{G}_J(\boldsymbol{q})\times\boldsymbol{J}_2(\boldsymbol{q}) \tag{13}$$

with

$$\boldsymbol{J}_2(\boldsymbol{q}) = \int_{\mathcal{R}_2} d^2\boldsymbol{\rho}e^{-i\boldsymbol{q}\cdot\boldsymbol{\rho}}\boldsymbol{J}_2(\boldsymbol{\rho}), \tag{14}$$

where the kernel is given as

$$\boldsymbol{G}_J(\boldsymbol{q}) = \frac{4\pi}{L_zqc}\sinh(L_zq/2)e^{-qd}\left(i\hat{\boldsymbol{q}}-\mathrm{sign}(d)\hat{\boldsymbol{z}}\right). \tag{15}$$

Again assuming $L_z\ll d$ we obtain

$$\boldsymbol{G}_J(\boldsymbol{q}) = \frac{2\pi}{c}e^{-qd}\left(i\hat{\boldsymbol{q}}-\mathrm{sign}(d)\hat{\boldsymbol{z}}\right). \tag{16}$$

C. NV sensor of material noise

The T_1^{-1} relaxation rate is related to material noise using Eq. (1), and the magnetic field at the height of the NV as determined above. The above kernels function then relate the magnetic field correlations to the correlations of the magnetization and current densities. To simplify these relations, we will assume the NV magnetic dipole moment has orientation perpendicular to the plane, such that $B^{\pm} = B^x \pm iB^y$. We will also assume a few properties on the current and magnetization. First, we assume current fluctuations are dominated by transverse fluctuations $\boldsymbol{J}(\boldsymbol{q})\cdot\boldsymbol{q} \approx 0$ which will be later justified. Second, we assume the magnetization comes solely from the electron spin and is isotropic. Under these assumptions the NV relaxation rate due to magnetization noise is given by

$$T_1^{-1} \propto \int \frac{d^2\boldsymbol{q}_1 d^2\boldsymbol{q}_2}{(2\pi)^4} q_1 q_2 e^{-(q_1+q_2)d} \int_{-\infty}^{\infty} dt e^{i\Delta t} \left\langle \{M^a(\boldsymbol{q}_1, t), M^a(\boldsymbol{q}_2, 0)\}\right\rangle . \tag{17}$$

For a finite system that is homogeneous inside the sample, the magnetization fluctuations $\langle\{M^a(\boldsymbol{q}_1, t), M^a(\boldsymbol{q}_2, 0)\}\rangle$ are strongly peaked at $\boldsymbol{q}_1 = -\boldsymbol{q}_2$. This peak diverges with system size, and in a translation invariant system, correlations of this form (i.e. $\langle f(\boldsymbol{q}_1)f(\boldsymbol{q}_2)\rangle$) are singular:

$$\langle f(\boldsymbol{q}_1)f(\boldsymbol{q}_2)\rangle = (2\pi)^2\delta(\boldsymbol{q}_1+\boldsymbol{q}_2)\int d\boldsymbol{r} e^{-i\boldsymbol{q}_1\cdot\boldsymbol{r}} \langle f(\boldsymbol{r})f(0)\rangle \tag{18}$$

with nonsingular part given by the Fourier transform of the auto correlation function. The nonsingular part is

$$\int d\boldsymbol{r} e^{-i\boldsymbol{q}\cdot\boldsymbol{r}} \langle f(\boldsymbol{r})f(0)\rangle = \lim_{V\to\infty}\frac{1}{V}\langle f_V(\boldsymbol{q})f_V(-\boldsymbol{q})\rangle = C_{ff}(\boldsymbol{q}), \tag{19}$$

where $f_V(\boldsymbol{q}) = \int_V e^{-i\boldsymbol{q}\cdot\boldsymbol{r}} f(r)$ is the finite volume Fourier transform.

The NV is therefore sensing the power spectral density of the magnetization and current noise. Explicitly, we find

$$T_1^{-1} \;=\; \left(\frac{g_{\mathrm{nv}}\mu_B}{2\hbar}\right)^2 \int d^2\boldsymbol{q} e^{-2dq}\left[2q^2 C_{\{M,M\}}(\boldsymbol{q},\omega) + \frac{1}{c^2}C_{\{J_\perp,J_\perp\}}(\boldsymbol{q},\omega)\right], \tag{20}$$

where the power spectral densities of the magnetization and transverse current noise are given as

$$\begin{aligned} C_{\{M,M\}}(\boldsymbol{q},\omega) \;&=\; \int dt e^{i\omega t}\lim_{V\to\infty}\frac{1}{V}\left\langle\{M_V^\alpha(\boldsymbol{q},t)M_V^\alpha(-\boldsymbol{q})\}\right\rangle \\ C_{\{J_\perp,J_\perp\}}(\boldsymbol{q},\omega) \;&=\; \int dt e^{i\omega t}\lim_{V\to\infty}\frac{1}{V}\left\langle\{J_{\perp,V}(\boldsymbol{q},t)J_{\perp,V}(-\boldsymbol{q})\}\right\rangle , \end{aligned} \tag{21}$$

where $J_\perp(\boldsymbol{q})$ is the current density component perpendicular to the wave vector $\boldsymbol{q}$.

D. Orientation dependence of NV

We now assume the NV points at an angle θ relative to normal of the material. Take the direction of the NV projected onto the material plane as the $\hat{\boldsymbol{x}}$ direction such that the dipole of the NV is

$$\hat{\boldsymbol{d}} = d(\cos\theta\hat{\boldsymbol{z}} + \sin\theta\hat{\boldsymbol{x}}) \tag{22}$$

Furthermore, we define $\hat{\boldsymbol{y}}$ to be perpendicular to the dipole and in the material plane, and define another vector $\hat{\boldsymbol{\alpha}}$ as

$$\hat{\boldsymbol{\alpha}} = \hat{\boldsymbol{y}}\times\hat{\boldsymbol{d}} = -\sin\theta\hat{z} + \cos\theta\hat{x}, \tag{23}$$

to construct a right-handed basis $\hat{\boldsymbol{d}}, \hat{\boldsymbol{\alpha}}, \hat{\boldsymbol{y}}$. See Fig. 1 for reference.

The relaxation rate due to current fluctuations in directions $\boldsymbol{v}_l$ and $\boldsymbol{v}_k$ is then

$$T_1^{-1} \;=\; \left(\frac{g_{\mathrm{nv}}\mu_B}{2\hbar}\right)^2 \int \frac{d^2\boldsymbol{q}}{(2\pi)^2}\sum_{kl}\left(\boldsymbol{n}_-\cdot\boldsymbol{G}_J(\boldsymbol{q})\times\hat{\boldsymbol{v}}_{\boldsymbol{k}}\right)\left(\boldsymbol{n}_+\cdot\boldsymbol{G}_J(-\boldsymbol{q})\times\hat{\boldsymbol{v}}_{\boldsymbol{l}}\right)C^{kl}_{\{J,J\}}(\omega,\boldsymbol{q}), \tag{24}$$

where $\hat{\boldsymbol{n}_\pm} = \hat{\boldsymbol{\alpha}} \pm i\boldsymbol{y}$

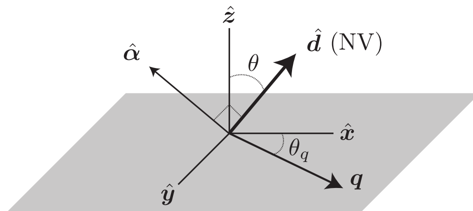

FIG. 1. The projection of $\hat{\boldsymbol{d}}$ on to the material plane (shown in gray) is in the $\hat{\boldsymbol{x}}$ direction. The vector $\boldsymbol{q}$ points in plane, and the vectors $\hat{\boldsymbol{d}}$, $\hat{\boldsymbol{\alpha}}$, and $\hat{\boldsymbol{y}}$ form a right-handed basis.

By neglecting contributions from longitudinal-current fluctuations, and only considered transverse-current fluctuations $C_{\{J_\perp,J_\perp\}} = \sum_{kl}(\hat{\boldsymbol{q}_\perp}\cdot\hat{\boldsymbol{v}_k})(\hat{\boldsymbol{q}_\perp}\cdot\hat{\boldsymbol{v}_l})C^{kl}_{\{J,J\}}(\omega,\boldsymbol{q})$, we obtain the relaxation rate as

$$T_1^{-1} = \left(\frac{g_{\rm nv}\mu_B}{2\hbar}\right)^2 \int \frac{qdqd\theta_q}{c^2} e^{-2dq} C_{\{J_\perp,J_\perp\}}(\omega,\boldsymbol{q}) f(\theta,\theta_q), \tag{25}$$

where

$$f(\theta,\theta_q) = \left(\cos\theta\cos\theta_q + i\left(\sin\theta_q - \sin\theta\right)\right)\left(\cos\theta\cos\theta_q - i\left(\sin\theta_q - \sin\theta\right)\right), \tag{26}$$

is the factor that depends on the NV orientation θ, and the angle θ_q formed by the vector $\boldsymbol{q}$ and the $\hat{\boldsymbol{x}}$ axis (See Fig. 1). For an NV pointing in the $\hat{\boldsymbol{z}}$ direction, $f(\theta,\theta_q) = 1$, while for an NV pointing in-plane $f(\theta) = (1-\sin\theta_q)^2$. When the current noise is isotropic, the integral over θ_q yields only a geometric factor

$$F_0(\theta) = \int_0^{2\pi} d\theta_q f(\theta,\theta_q) = \frac{1}{2}\pi(5 - cos(2\theta)). \tag{27}$$

In contrast, if the current fluctuations are anisotropic, depending on θ_q, then the in-plane angle dependence of the NV can be used to resolve that anisotropy. Suppose now that the material is rotated by an angle ϕ around the $\hat{\boldsymbol{z}}$ axis. The NV relaxation rate is now given as

$$T_1^{-1}(d,\omega,\phi) = \left(\frac{g_{\rm nv}\mu_B}{2\hbar}\right)^2 \int \frac{qdqd\theta_q}{c^2} e^{-2dq} C_{\{J_\perp,J_\perp\}}(\omega,\boldsymbol{q}) f(\theta,\theta_q-\phi), \tag{28}$$

Decomposing the noise in circular harmonics $C_{\{J_\perp,J_\perp\}}(\omega,q,\theta_q) = \sum_n C_{\{J_\perp,J_\perp\}}(\omega,q,n)e^{in\theta_q}$, we can compute the geometric factor for each harmonic:

$$T_1^{-1}(d,\omega,\phi) = \left(\frac{g_{\rm nv}\mu_B}{2\hbar}\right)^2 \sum_n F_n(\theta,\phi) \int \frac{qdq}{c^2} e^{-2dq} C_{\{J_\perp,J_\perp\}}(\omega,q,n), \tag{29}$$

where $F_n(\theta,\phi) = \int d\theta_q e^{in\theta_q} f(\theta,\theta_q-\phi)$. Since $f(\theta,\theta_q)$ is real, the geometric factors satisfy $F_n^* = F_{-n}$. Since f is a polynomial in trigonometic functions of degree 2, $F_n(\theta,\phi) = 0$ for $|n| > 2$, such that a single NV is only sensitive to the $n \in [-2,2]$ harmonics. The geometric factor for the first and second angular harmonics are

$$\begin{aligned} F_1(\theta,\phi) &= 2\pi\sin\theta(\sin\phi - i\cos\phi) \\ F_2(\theta,\phi) &= -\frac{1}{2}\pi e^{2i\phi}\sin^2\theta \end{aligned} \tag{30}$$

which notably depends on the orientation of the NV.

II. BALLISTIC NOISE IN THE NORMAL STATE

In this appendix we review the current and magnetization noise of a noninteracting Fermi gas, and then relate them to the T_1^{-1} relaxation rate of the NV.

A. Current noise

For a fixed 2D volume, V, the current density at wave vector $\boldsymbol{q}$ has the form

$$\boldsymbol{J}(\boldsymbol{q}) = \int_V d\boldsymbol{\rho} e^{-i\boldsymbol{q}\cdot\boldsymbol{\rho}} \boldsymbol{J}(\boldsymbol{\rho}) = \frac{e\hbar}{m} \sum_{\sigma,\boldsymbol{k}} (\boldsymbol{k} - \frac{\boldsymbol{q}}{2}) f^\dagger_{\sigma,\boldsymbol{k}-\boldsymbol{q}} f_{\sigma,\boldsymbol{k}}, \tag{31}$$

and the auto correlation of the magnetic noise is therefore

$$C_{\{\boldsymbol{J},\boldsymbol{J}\}}(\boldsymbol{q},\omega) = \left(\frac{e\hbar}{m}\right)^2 \lim_{V\to\infty} \frac{1}{V} \sum_{\boldsymbol{k},\boldsymbol{k}',\sigma,\sigma'} \int dt e^{i\omega t} \left(\boldsymbol{k} - \frac{\boldsymbol{q}}{2}\right)\left(\boldsymbol{k}' + \frac{\boldsymbol{q}}{2}\right) \left\langle \left\{ f^\dagger_{\sigma,\boldsymbol{k}-\boldsymbol{q}}(t) f_{\sigma,\boldsymbol{k}}(t), f^\dagger_{\sigma',\boldsymbol{k}'+\boldsymbol{q}} f_{\sigma',\boldsymbol{k}'} \right\} \right\rangle. \tag{32}$$

After applying the commutation rules for fermion operators this expression equates to

$$C_{\{\boldsymbol{J},\boldsymbol{J}\}}(\boldsymbol{q},\omega) = 2\left(\frac{e\hbar}{m}\right)^2 \int \frac{d\boldsymbol{k}}{2\pi} \delta\left(\omega - E_{\boldsymbol{k}-\boldsymbol{q}}/\hbar + E_{\boldsymbol{k}}/\hbar\right) \left(\boldsymbol{k} - \frac{\boldsymbol{q}}{2}\right)^2 \left(n_{\boldsymbol{k}-\boldsymbol{q}}\left(1-n_{\boldsymbol{k}}\right) + \left(1-n_{\boldsymbol{k}-\boldsymbol{q}}\right) n_{\boldsymbol{k}}\right), \tag{33}$$

which scales as $(e\hbar k_F/m_e)^2 = (ev_F)^2$ and with the number of particle-hole pairs near the Fermi surface and with energy difference, $\hbar\omega$ and momenta difference $\hbar\boldsymbol{q}$.

The number of such pairs is severely restricted when $\hbar\omega \ll E_F$ and $\hbar\boldsymbol{q} \ll \hbar k_F$, which is the case for the NV relaxation process. In particular, only particles and holes with an energy $|E_F - E| < k_B T$ near the Fermi surface contribute, while current fluctuations with $q > 1/d$ are suppressed by the kernel relating the magnetic field to the material current. Thus, we evaluate the constraint by expanding $E_{\boldsymbol{k}-\boldsymbol{q}}$ around $\boldsymbol{k}$: $\omega = \boldsymbol{v_g}(\boldsymbol{k})\cdot\boldsymbol{q}$, where $\boldsymbol{v_g} = \boldsymbol{\nabla_k} E_k = \hbar\boldsymbol{k}/2m$ is the group velocity. When $\omega/v_F q$ is small, the constraint enforces $\hat{\boldsymbol{k}}\cdot\hat{\boldsymbol{q}} \ll 1$ such that only transverse currents contribute. For NV frequency in the GHz range, and Fermi velocity $v_F \approx 10^6$ m/s, this condition corresponds to $q > 10^3$ m^{-1}. This condition holds for the wave numbers probed by the NV, $q \approx 1/d \in (10^6, 10^9)$ m^{-1}.

Under these approximations, we find the current spectral density to be

$$C^N_{\{J_\perp,J_\perp\}}(\boldsymbol{q},\omega) = 4(ev_F)^2 n_e \frac{k_B T}{E_F} \frac{1}{v_F q}, \tag{34}$$

where $n_e = k_F^2/2\pi$ is the electron density. Furthermore, we have assumed $\hbar\omega \ll k_B T$ so that we can approximate $n_{\boldsymbol{k}-\boldsymbol{q}} \approx n_{\boldsymbol{k}}$.

B. Spin noise

The magnetization carried by the conduction electrons has a form:

$$\boldsymbol{M}(\boldsymbol{q}) = \int_V d\boldsymbol{\rho} e^{-i\boldsymbol{q}\cdot\boldsymbol{\rho}} \boldsymbol{M}(\boldsymbol{r}) = \mu_B \sum_{\sigma,\sigma',\boldsymbol{k}} \boldsymbol{\sigma}_{\sigma,\sigma'} f^\dagger_{\sigma,\boldsymbol{k}-\boldsymbol{q}} f_{\sigma',\boldsymbol{k}}. \tag{35}$$

Thus, the magnetization noise will be similar to the current noise except now the matrix elements are proportional to $\boldsymbol{\sigma}$ instead of $\boldsymbol{k}-\boldsymbol{q}$. In the limit of small frequencies, $\omega \ll v_F q$, the current matrix elements are fixed $\boldsymbol{k}-\boldsymbol{q} \approx k_F \hat{\boldsymbol{q}}_\perp$ perpendicular to the wave vector $\boldsymbol{q}$. Thus, the matrix elements for the current operator are also effectively independent of the momenta of the particle-hole pairs. The only other difference between the two is that the magnetization noise involves a spin flip, and so there is an overall factor of two relative to the current noise, in which spin is just a degeneracy. We conclude that the magnetization noise is related to the current noise by a constant factor:

$$C_{\{M,M\}}(\boldsymbol{q},\omega) = \frac{1}{2}\left(\frac{m\mu_B}{e\hbar k_F}\right)^2 C_{\{J_\perp,J_\perp\}}(\boldsymbol{q},\omega). \tag{36}$$

C. Comparison

The magnetic field noise produced by the current noise is $N_J(\boldsymbol{q},\Delta) = C_{JJ}(\boldsymbol{q},\Delta)/c^2$, while that produced by the magnetization noise is $N_M(\boldsymbol{q},\Delta) = 2q^2 C_{MM}(\boldsymbol{q},\Delta)$ with a ratio

$$\frac{N_M(\boldsymbol{q},\Delta)}{N_J(\boldsymbol{q},\Delta)} = c^2 q^2 \left(\frac{m\mu_B}{e\hbar k_F}\right)^2 = \left(\frac{q}{2k_F}\right)^2. \tag{37}$$

Since the magnetic propagator suppresses wave numbers $q > 1/d$ and $1/d \ll k_f$, current contribution generally dominates the magnetization contribution. Spin noise will become relevant if the system has a small Fermi surface (i.e. $1/k_f \approx 100nm$) and the NV is very close to the sample. In this case, the small q expansions performed above would be invalid. Here, we briefly mention a similar comparison was found in Ref. [6], but for an analysis done in the diffusive limit. In that case, other factors such as the scattering length, and the spin lifetime, can also affect the condition for spin noise to dominate current noise.

III. BCS MODEL

To model the magnetization and current fluctuations, we assume the superconductor can be described by the BCS Hamiltonian

$$H = \sum_{\boldsymbol{k},\sigma} \xi_k f^\dagger_{\boldsymbol{k},\sigma} f_{\boldsymbol{k},\sigma} + \sum_{kl} V_{\boldsymbol{k},\boldsymbol{l}} f^\dagger_{\boldsymbol{k},\uparrow} f^\dagger_{-\boldsymbol{k},\downarrow} f_{-\boldsymbol{l},\downarrow} f_{\boldsymbol{l},\uparrow} + h.c. \, , \tag{38}$$

where $f^\dagger_{\boldsymbol{k},\sigma}$ is the fermion creation operator with momentum $\boldsymbol{k}$ and spin σ, $\xi_k = \hbar^2 k^2/2m$ is the dispersion and $V_{\boldsymbol{k},\boldsymbol{l}}$ is the pairing interaction. We follow the usual BCS treatment and assume interaction of the form $V_{\boldsymbol{k},\boldsymbol{l}} = -V\theta(\hbar\omega_D - \xi_{\boldsymbol{k}})\theta(\hbar\omega_D - \xi_{\boldsymbol{l}})$ where ω_D is the Debye frequency of the phonons.

Interactions of this form are accurately captured by a mean field approximation in which the s-wave superconducting order parameter $\Delta = -\sum_{\boldsymbol{l}} V_{\boldsymbol{k},\boldsymbol{l}} \langle f_{-\boldsymbol{l},\downarrow} f_{\boldsymbol{l},\uparrow}\rangle$, can be determined self consistently. The mean field Hamiltonian is then diagonalized with quasiparticle energy $E_k = +\sqrt{(\xi_k - E_F)^2 + \Delta^2}$, by the canonical transformation

$$\begin{aligned} f_{\boldsymbol{k},\uparrow} &= u_k \gamma_{\boldsymbol{k},\uparrow} + v_k \gamma^\dagger_{-\boldsymbol{k},\downarrow} \\ f_{-\boldsymbol{k},\downarrow} &= u_k \gamma_{-\boldsymbol{k},\downarrow} - v_k \gamma^\dagger_{\boldsymbol{k},\uparrow}, \end{aligned} \tag{39}$$

where $u_k = \cos(\theta_k/2)$, $v_k = \sin(\theta_k/2)$, E_F is the Fermi energy, and $\sin(\theta_k) = \Delta/E_k$ and $\cos(\theta_k) = \xi_k/E_k$.

In the superconducting phase, quasiparticle states only exist for energies above the gap $E > \Delta$ and have a square-root singularity

$$D_{SC}(E) = \frac{1}{2}\int \frac{d^2\boldsymbol{k}}{(2\pi)^2}\delta(E - E(k)) = D_n \frac{E}{\sqrt{E^2 - \Delta^2}}, \tag{40}$$

for relevant $E < \sqrt{E_f^2 + \Delta^2}$ and where D_n is the constant $2D$ normal-state density of states $D_n = m/(2\pi\hbar^2) = n_e/E_F = (\hbar v_F 2\pi/k_F)^{-1}$ at the Fermi surface. Notice, that for $E < \sqrt{E_f^2 + \Delta^2}$, the equation $E = E(k)$ has two solutions corresponding to whether $\xi_k - E_F$ is greater or smaller than 0. The factor of 1/2 in the definition of $D_{SC}(E)$ is so that only one solution is counted. This singularity originates from the vanishing group velocity of the superconducting quasiparticles at the Fermi surface $\hbar v_g|_{k_F} = \boldsymbol{\nabla}_{\boldsymbol{k}} E_k|_{k_F} = 0$.

A. Time reversal and the coherence peak

In this section we show, for an s-wave superconductor, that the coherence peak in the noise of an observable requires that the observable is odd under time reversal. Under time reversal, a general observable

$$O = \sum_{\boldsymbol{k},\boldsymbol{k}',\sigma,\sigma'} O^{\sigma,\sigma'}_{\boldsymbol{k},\boldsymbol{k}'} f^\dagger_{\boldsymbol{k},\sigma} f_{\boldsymbol{k}',\sigma'} \tag{41}$$

transforms as

$$TOT^{-1} = \sum_{\boldsymbol{k},\boldsymbol{k}'} \sigma\sigma' O^{\bar{\sigma},\bar{\sigma}'*}_{-\boldsymbol{k},-\boldsymbol{k}'} f^\dagger_{\boldsymbol{k},\sigma} f_{\boldsymbol{k}',\sigma'}, \tag{42}$$

where $\bar{\sigma}$ indicates the opposite spin from $\sigma \in \{\uparrow,\downarrow\}$, and T is the anti-unitary time-reversal operator. If the observable is Hermitian, then we have

$$TOT^{-1} = \sum_{\boldsymbol{k},\boldsymbol{k}'} \sigma\sigma' O^{\bar{\sigma}',\bar{\sigma}}_{-\boldsymbol{k}',-\boldsymbol{k}} f^\dagger_{\boldsymbol{k},\sigma} f_{\boldsymbol{k}',\sigma'}. \tag{43}$$

Furthermore, if the observable is odd (or even) under time reversal then $TOT^{-1} = \mp O$ and

$$O^{\sigma,\sigma'}_{\boldsymbol{k},\boldsymbol{k}'} = \mp\sigma\sigma' O^{\bar{\sigma}',\bar{\sigma}}_{-\boldsymbol{k}',-\boldsymbol{k}}. \tag{44}$$

In the quasiparticle basis, the observable has the form

$$O = \sum_{\boldsymbol{k},\boldsymbol{k}',\sigma,\sigma'} \left[O^{\sigma,\sigma'}_{\boldsymbol{k},\boldsymbol{k}'} u_{\boldsymbol{k}} u_{\boldsymbol{k}'} - \sigma\sigma' O^{\bar{\sigma}',\bar{\sigma}}_{-\boldsymbol{k}',-\boldsymbol{k}} v_{\boldsymbol{k}} v_{\boldsymbol{k}'} \right] \gamma^\dagger_{\boldsymbol{k},\sigma}\gamma_{\boldsymbol{k}',\sigma'}, \tag{45}$$

where we have neglected pair creation and annihilation $\propto \gamma^\dagger\gamma^\dagger$ terms. For energies near the gap, $|\boldsymbol{k}| \approx k_F$, the quasiparticle weights become identical $v_k \approx u_k \approx 1/\sqrt{2}$. In this region of single-particle Hilbert space, the observable will have significant contributions only if

$$O^{\sigma,\sigma'}_{\boldsymbol{k},\boldsymbol{k}'} - \sigma\sigma' O^{\bar{\sigma}',\bar{\sigma}}_{-\boldsymbol{k}',-\boldsymbol{k}} \neq 0, \tag{46}$$

which is guaranteed by Eq. (44) for observables that are odd under time reversal $TOT^{-1} = -O$, and is impossible for observables that are even under time reversal. Since the singular density of states occurs for $E \to \Delta$, only observables which are odd under time reversal will be sensitive to the singularity and show a coherence peak.

IV. BALLISTIC CURRENT NOISE IN A SUPERCONDUCTOR

For a superconductor, the current noise has similar structure to the normal state except for a few key differences. The first is that, in principle, the current noise in a superconductor has contributions from the breaking and reforming of Cooper pairs. These contributions only occur when $\hbar\omega > 2\Delta$ which is not the case for the experiment. In the experiment [13], the gap is around 10K, while the NV frequency is around 2GHz, and so this condition is never met. The second difference is that the quasi-particles are not directly related to bare electrons. While the final, most important difference, is that the dispersion has dramatically changed.

Thus, we similarly consider the current spectral density

$$C_{\{\boldsymbol{J},\boldsymbol{J}\}} = 2\left(\frac{e\hbar}{m}\right)^2 \int \frac{d^2\boldsymbol{k}}{2\pi}\left(\boldsymbol{k} - \frac{\boldsymbol{q}}{2}\right)^2 F_+\left(E_k, E_{k-q}\right)\delta\left(\omega - E_{\boldsymbol{k}-\boldsymbol{q}}/\hbar + E_{\boldsymbol{k}}/\hbar\right)\left[n_{\boldsymbol{k}-\boldsymbol{q}}\left(1-n_{\boldsymbol{k}}\right) + \left(1-n_{\boldsymbol{k}-\boldsymbol{q}}\right)n_{\boldsymbol{k}}\right], \tag{47}$$

where the coherence factor is given as

$$F_+(E_k, E_{k-q}) = \left(u_{\boldsymbol{k}} u_{\boldsymbol{k}-\boldsymbol{q}} + v_{\boldsymbol{k}} v_{\boldsymbol{k}-\boldsymbol{q}}\right)^2 \approx \frac{1}{2}\left(1 + \frac{\Delta^2}{E_{\boldsymbol{k}} E_{\boldsymbol{k}-\boldsymbol{q}}}\right), \tag{48}$$

and the approximation holds when $\sqrt{E^2_{\boldsymbol{k}} - \Delta^2}\sqrt{E^2_{\boldsymbol{k}-\boldsymbol{q}} - \Delta^2} \ll \Delta^2$.

Instead of immediately expanding the constraint in small q/k_f, as done for the normal state, we will first formally integrate θ_k and make the change of variables from $|\boldsymbol{k}| \to (E, s)$. The additional variable $s = \pm 1$ is required because the transform from energy coordinates $\xi_{\boldsymbol{k}} = E_F + s\sqrt{E^2 - \Delta^2}$ is multivalued. Likewise, the constraint has two solutions for $\sin\theta_c$ (4 solutions for θ_c) for a fixed $|\boldsymbol{k}|$. Thus, for a fixed energy $E_{\boldsymbol{k}}$, there are at most eight, $c = 1..8$, particle-hole pairs which contribute to the current noise. For each of these possible contributions, the integral over θ_k yields

$$\int d\theta_k \delta\left(\omega - E_{\boldsymbol{k}-\boldsymbol{q}}/\hbar + E_{\boldsymbol{k}}/\hbar\right) \to \hbar\left|\partial_{\theta_k} E_{\boldsymbol{k}-\boldsymbol{q}}\right|^{-1} = D_{SC}(E_k + \hbar\omega)\frac{2\pi\hbar}{k_c q\left|\sin\theta_c\right|}, \tag{49}$$

where $k_c = |\boldsymbol{k}|\,(E_k, c)$ is one of the momenta fixed by the energy E_k, while θ_c is one of the solution for $\theta_k - \theta_q$.

Using this change of variables the current spectral density is now

$$C^{SC}_{\{J_\perp,J_\perp\}} = 4\pi(ev_F)^2 \int dE D_{SC}(E) D_{SC}(E+\hbar\omega) F_+(E, E+\hbar\omega) f_n(E,\hbar\omega,k_BT)\sum_c \frac{\hbar\left|\sin\theta_c\right|}{k_c q}, \tag{50}$$

where $f_n(E,\hbar\omega,k_BT) = \left[n_{\boldsymbol{k}-\boldsymbol{q}}\left(1-n_{\boldsymbol{k}}\right) + \left(1-n_{\boldsymbol{k}-\boldsymbol{q}}\right)n_{\boldsymbol{k}}\right]$ contains the dependence on the density of fermions. This form is similar to the contribution to the spin noise sensed by a nuclear spin (see below) except for the sum over the eight possible particle-hole pairs, c, and the dependence on $\boldsymbol{q}$ and $\sin\theta_c$ (also depends on $\boldsymbol{q}$).

For $\xi_{\boldsymbol{k}} = E_F \left|\boldsymbol{k}\right|^2 / k_F^2$, the solution to the constraint is given by

$$2\tilde{k}_c \tilde{q} \cos\theta_c = \tilde{k}_c^2 - 1 + \tilde{q}^2 \pm \frac{1}{E_F}\sqrt{(\hbar\omega + E_{\boldsymbol{k}})^2 - \Delta^2}, \tag{51}$$

where $\tilde{q} = q/k_F$ and $\tilde{k}_c = k_c/k_F$. The eight particle-hole pairs come from the two choices for $\tilde{k}_c$, the choice between the $\pm$ solution, and two choices for the sign of θ_c. Depending on $\boldsymbol{q}$ and $\boldsymbol{k}$, one or more of these pairs do not have a valid solution for θ_c. In these limits, the pair does not contribute to the current spectral density.

With these solutions, we find the enhancement of the spectral density of the superconductor's current noise, $R_J(\omega, \boldsymbol{q}) = C^{SC}_{\{J_\perp, J_\perp\}} / C^{N}_{\{J_\perp, J_\perp\}}$, relative to the normal-state result is given by

$$R_J(\omega, \boldsymbol{q}, T, \Delta) = \frac{1}{4k_BT}\int_{\Delta}^{\infty} dE \frac{E}{\sqrt{E^2 - \Delta^2}} \frac{E + \hbar\omega}{\sqrt{\left(E + \hbar\omega\right)^2 - \Delta^2}} F_+(E, E + \hbar\omega) f_n(E) \sum_c \frac{k_F}{k_c}\sin\theta_c, \tag{52}$$

while the enhancement of the relaxation rate $R_1(\omega, d, T) = T^{-1}_{1,SC}/T^{-1}_{1,N}$ is given by

$$R_1(\omega, d, T, \Delta) = 2d\int dq e^{-2dq} R_J(\omega, q, T, \Delta). \tag{53}$$

A. The log singularity at low frequency

For vanishing NV frequency, $\omega \to 0$, the integrand in Eq. (52) diverges as $(E - \Delta)^{-1}$ for energies, $E \to \Delta$ close to the gap. For finite but small frequencies $\hbar\omega \ll 1$, the integral convergences but is large in $\ln(\hbar\omega/\Delta)$. This follows by splitting the integral into two parts, one for $E < \Delta/(1 - \hbar\omega/\Delta)$, and another for $E > \Delta/(1 - \hbar\omega/\Delta)$. In the first limit, the integrand is approximately constant in energy except for a square root singularity:

$$\frac{1}{4k_BT} F_+(E, E + \hbar\omega) f_n(E) \sum_c \frac{k_F}{k_c}\sin\theta_c \sqrt{\frac{\Delta}{2\hbar\omega}} \int_{\Delta}^{\frac{\Delta^2}{\Delta - \hbar\omega}} dE \frac{E}{\sqrt{E^2 - \Delta^2}}. \tag{54}$$

The integral is convergent and not scaling with $\hbar\omega$. In the second limit, the integrand scales with $E^2/(E^2 - \Delta^2) = E^2/(E - \Delta)(E + \Delta)$ and results in the integral scaling logarithmically as $\ln(\Delta/\hbar\omega)$.

B. Height and momentum dependence

The enhancement of current noise depends on the wave number $|\boldsymbol{q}|$. In particular, the angle θ_c, and number of particle-hole pairs that solve the kinematic constraint depends on $\boldsymbol{q}$ (See main text for a cartoon demonstration). This dependence also occurs for a normal-state Fermi gas in which two limits arise: 1) when $|\boldsymbol{q}| > 2k_F$ and 2) when $|\boldsymbol{q}| < k_F\hbar\omega/E_F$. In the first limit, the particle-hole pairs cannot be created both on the Fermi surface, while in the second limit the momentum difference of particle-hole pairs is too small to be separated by an energy $\hbar\omega$.

In the superconductor, the coherence length $\xi_0 = 2E_F/\pi\Delta k_F$ is a new length scale, above which the phase space for solutions to the kinetic constraint in Eq. (51) is reduced. Specifically, the phase space is reduced for solutions for which $\boldsymbol{k}$ and $\boldsymbol{k} - \boldsymbol{q}$ are on opposite sides of the Fermi surface. These type of solutions require

$$E_{\boldsymbol{k}} < \frac{1}{2}\sqrt{E_F^2 (q/k_F)^2 + \Delta^2} \tag{55}$$

This constraint to phase space doesn't matter for larger q or for small temperatures, since quasiparticles are suppressed for energies $E_{\boldsymbol{k}} \gg k_BT$. Thus, this constraint is only relevant when $\frac{1}{2}\sqrt{E_F^2(q/k_F)^2 + \Delta^2} \approx k_BT \approx \Delta$, or when $q \lesssim \xi_0^{-1}$.

For smaller q, Eq. 55 sets a new upper bound on the noise integral . The integral still yields a logarithm, but with a new upper bound that is shrinking as $(q\xi_0)^2$. Thus, we conclude that the scaling of the integral is therefore $\ln\big((q\xi_0)^2\Delta/\omega\big)$, which is confirmed by the numerical results for the NV relaxation shown in the main text.

C. Comparison with nuclear spin relaxation

In contrast, nuclear spins relax due to the local spin noise

$$C_{\{\boldsymbol{M},\boldsymbol{M}\}}(\boldsymbol{\rho}=0,\omega)=\int\frac{d^2\boldsymbol{q}}{(2\pi)^2}C_{\{\boldsymbol{M},\boldsymbol{M}\}}(\boldsymbol{q},\omega), \tag{56}$$

where the important difference is the nuclear spin is sensitive to noise at all length scales. The spin noise, $C_{\{\boldsymbol{M},\boldsymbol{M}\}}$, has a similar form to the current density noise in Eq. (47). Upon integral over scattering momenta $\boldsymbol{q}$, momentum conservation is relaxed and we find

$$\int\frac{d^2\boldsymbol{q}}{(2\pi)^2}C_{\{\boldsymbol{M},\boldsymbol{M}\}}(\boldsymbol{q},\omega)=8\pi\mu_B^2\,\mathrm{tr}\left[\boldsymbol{\sigma}\boldsymbol{\sigma}\right]\int dE_1dE_2D_{SC}(E_1)D_{SC}(E_2)\delta(\hbar\omega-E_1+E_2)F_+(E_1,E_2)f_n\left(E_1,\hbar\omega,k_BT/\Delta\right).$$

Similar to the NV relaxation rate, we can express the ratio between the normal state and superconducting state relaxation as:

$$\frac{T_{1,SC}^{-1}}{T_{1,N}^{-1}}=\frac{1}{k_BT}\int_\Delta^\infty dE\frac{E}{\sqrt{E^2-\Delta^2}}\frac{(E+\hbar\omega)}{\sqrt{(E+\hbar\omega)^2-\Delta^2}}\left(1+\frac{\Delta}{E\left(E+\hbar\omega\right)}\right)f_n\left(E,\hbar\omega,k_BT/\Delta\right). \tag{57}$$

Similar to the case of long wavelength magnetic noise, the local spin noise is an integral over a singular density of states, and the integral diverges for $\hbar\omega/\Delta\to0$. The difference is in the lack of height dependence that simplifies the expression.

D. Dependence on Fermi-surface size

The noise captured by the isotropic BCS theory depends on only a few parameters: the critical temperature T_c, the NV frequency ω, the Fermi energy E_F and the Fermi wavelength $2\pi/k_F$. The BCS coherence length at a given temperature is then given by $\xi(T)=2E_F/\pi\Delta(T)k_F$. In Fig. 2, we plot the temperature dependence of the relative enhancement $R_1=\frac{T_{1,SC}^{-1}}{T_{1,N}^{-1}}$ for a few values of the zero-temperature coherence length ξ_0 obtained by varying k_F.

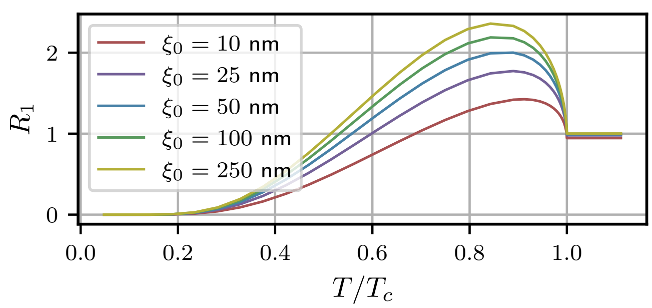

FIG. 2. Relative enhancement in T_1 as a function of temperature at a NV distance $d=100$ nm, a critical temperature $T_c=9K$, and Fermi energy $6*10^4K$. The legend shows the zero-temperaurte coherence length ξ_0. The curves show a sizable enhancement in the superconducting noise that decreases with decreasing ξ_0. For smaller coherence lengths (smaller Fermi wavelengths), the NV will need to be placed closer to the sample to observe the coherence peak. The zero temperature coherence length ξ_0 is shown in the legend.

[1] B. Flebus and Y. Tserkovnyak, Quantum-Impurity Relaxometry of Magnetization Dynamics, Physical Review Letters **121**, 187204 (2018).
[2] J. F. Rodriguez-Nieva, K. Agarwal, T. Giamarchi, B. I. Halperin, M. D. Lukin, and E. Demler, Probing one-dimensional systems via noise magnetometry with single spin qubits, Phys. Rev. B **98**, 195433 (2018).

[3] S. Chatterjee, P. E. Dolgirev, I. Esterlis, A. A. Zibrov, M. D. Lukin, N. Y. Yao, and E. Demler, Single-spin qubit magnetic spectroscopy of two-dimensional superconductivity, Physical Review Research **4**, L012001 (2022).

[4] P. E. Dolgirev, S. Chatterjee, I. Esterlis, A. A. Zibrov, M. D. Lukin, N. Y. Yao, and E. Demler, Characterizing two-dimensional superconductivity via nanoscale noise magnetometry with single-spin qubits, Phys. Rev. B **105**, 024507 (2022).

[5] H. Fang, S. Zhang, and Y. Tserkovnyak, Generalized model of magnon kinetics and subgap magnetic noise, Phys. Rev. B **105**, 184406 (2022).

[6] S. Zhang and Y. Tserkovnyak, Flavors of Magnetic Noise in Quantum Materials, Physical Review B **106**, L081122 (2022), arXiv:2108.07305 [cond-mat].

[7] J. Y. Khoo, F. Pientka, P. A. Lee, and I. S. Villadiego, Probing the quantum noise of the spinon fermi surface with nv centers, Phys. Rev. B **106**, 115108 (2022).

[8] J. Zou, S. Zhang, and Y. Tserkovnyak, Bell-state generation for spin qubits via dissipative coupling, Physical Review B **106**, L180406 (2022).

[9] J. B. Curtis, N. Maksimovic, N. R. Poniatowski, A. Yacoby, B. Halperin, P. Narang, and E. Demler, Probing the berezinskii-kosterlitz-thouless vortex unbinding transition in two-dimensional superconductors using local noise magnetometry, Phys. Rev. B **110**, 144518 (2024).

[10] X. Li, J. Marino, D. E. Chang, and B. Flebus, A solid-state platform for cooperative quantum dynamics driven by correlated emission (2024), arXiv:2309.08991 [quant-ph].

[11] K. Agarwal, R. Schmidt, B. Halperin, V. Oganesyan, G. Zaránd, M. D. Lukin, and E. Demler, Magnetic noise spectroscopy as a probe of local electronic correlations in two-dimensional systems, Phys. Rev. B **95**, 155107 (2017).

[12] K. Y. Guslienko and A. N. Slavin, Magnetostatic Green's functions for the description of spin waves in finite rectangular magnetic dots and stripes, Journal of Magnetism and Magnetic Materials **323**, 2418 (2011).

[13] S. Li, S. P. Kelly, J. Zhou, H. Lu, Y. Tserkovnyak, H. Wang, and C. R. Du, Observation of on- and off-resonant interaction between a solid-state spin qubit and a superconducting resonator (2024), arXiv:2412.18896 [cond-mat.mes-hall].